Atmos. Chem. Phys. Discuss., https://doi.org/10.5194/acp-2017-473
Manuscript under review for journal Atmos. Chem. Phys.
Discussion started: 2 June 2017

Regional severe particle pollution and its association with synoptic weather patterns in the Yangtze River Delta region, China

Lei Shu [1], Min Xie [1*], Da Gao [1], Tijian Wang [1*], Dexian Fang [2], Qian Liu [3], Anning Huang [1], Liwen Peng [1]

[1] School of Atmospheric Sciences, CMA-NJU Joint Laboratory for Climate Prediction Studies, Jiangsu Collaborative Innovation Center for Climate Change, Nanjing University, Nanjing 210023, China

[2] Chongqing Institute of Meteorology and Science, Chongqing 401147, China

[3] Jiangsu Provincial Academy of Environmental Science, Nanjing 210036, China

---

∗Corresponding to Min Xie (minxie@nju.edu.cn) and Tijian Wang (tjwang@nju.edu.cn)

Abstract: Regional air pollution is significantly associated with the dominant weather systems. In this study, the relationship between the particle pollution over the Yangtze River Delta (YRD) region and the weather patterns is investigated. Firstly, the pollution characteristics of particles ($PM_{2.5}$ and PM_{10}) in YRD are studied by using the in situ monitoring data in 16 cities from December 2013 to November 2014. The results show that the annual average concentrations in the cities of Jiangsu Province all exceed the national air quality standard. The pollution level is higher in the inland areas. Highest values can be found in Nanjing, with the concentrations of $PM_{2.5}$ and PM_{10} being 79 μg·m^{-3} and 130 μg·m^{-3}, respectively. The $PM_{2.5}/PM_{10}$ ratios are usually high in YRD, indicating that $PM_{2.5}$ is the overwhelmingly dominant particle pollutant. The wintertime peak of particle concentrations is tightly linked to the increased emissions in the heating season and the poor meteorological condition. Secondly, based on NCEP reanalysis data, synoptic weather classification is conducted to reveal that the weather patterns are easy to cause heavy pollution in YRD. Five typical synoptic patterns are objectively identified, including the East Asian trough rear pattern, the depression inverted trough pattern, the transversal trough pattern, the high-pressure controlled pattern, and the northeast cold vortex pattern. Finally, synthetic analysis of meteorological fields and backward trajectory calculation are used to further clarify

Atmos. Chem. Phys. Discuss., https://doi.org/10.5194/acp-2017-473
Manuscript under review for journal Atmos. Chem. Phys.
Discussion started: 2 June 2017

how these patterns impact particle concentrations. It is clarified that YRD is largely influenced by polluted air masses from the northern and the southern inland areas when it is at the rear of the East Asian major trough. In this case, the strong northwest wind hinders the vertical outward transport of pollutants. Thus, the East Asian trough rear pattern is quite favorable for the accumulation of pollutants in YRD, and respectively contributes 70.4% and 78.3% to the occurrence of large-scale regional $PM_{2.5}$ and PM_{10} pollution episodes. While under the weather systems for other patterns, the clean marine air masses may play great roles in the mitigation of particle pollution in YRD. The correlation between weather patterns and particle pollution can provide valuable views in the decision-making on pollution control and mitigation strategies.

Keywords: $PM_{2.5}$; PM_{10}; air pollution meteorology; synoptic weather pattern; the Yangtze River Delta region

1. Introduction

The high occurrence of regional particle pollution is acquired worldwide attention in the scientific community (Malm et al., 1994; Putaud et al., 2004; Chan and Yao, 2008) due to its adverse impacts on visibility (Singh and Dey, 2012; Green et al., 2012) and public health (Kappos et al., 2004; Brook et al., 2010). The causes for this kind of pollution involve diverse aspects. Among them, the emission of pollutants and weather conditions are two major contributors (Oanh and Leelasakultum, 2011; Young et al., 2016). Particle pollution in urban agglomerations is primarily attributed to the huge amounts of anthropogenic emission of primary particles and other precursors (SO_2, NO_x, and VOCs, etc.). However, the emission source groups are normally quasi-stable within a certain period of time (Kurokawa et al., 2013). Thus, the pollution level in a certain region generally depends on the regional weather conditions (weather patterns), which are strongly correlated with the synoptic-scale atmospheric circulation (Buchanan et al., 2002; Chuang et al., 2008; Flocas et al., 2009; Zhang et al., 2012; Zhao et al., 2013; Russo et al., 2014; Grundstrom et al., 2015; Zheng et al., 2015a; 2015b; Li et al., 2016).

Until now, researchers have gained improved knowledge of the relationship between weather patterns and particle pollution. For example, Buchanan et al. (2002) observed the significantly elevated concentrations of Black Smoke and PM_{10} under the anti-cyclonic, southerly and southeasterly weather types in the city of Edinburgh in UK between 1981 and 1996. Russo et al. (2014) showed an objective classification scheme of the atmospheric circulation affecting Portugal between 2002 and 2010, and revealed that higher concentrations of PM_{10}, O_3 and NO_2 are predominantly associated with synoptic circulation characterized by an eastern component and advection of dry air masses. Previous studies have confirmed that the levels of air pollution have close relations with weather patterns, and also showed great spatial variability ascribed to that the dominant weather pattern differs among different regions (Flocas et al., 2009; Grundstrom et al., 2015).

In recent decades, the air pollution caused by PM_{10} and $PM_{2.5}$ has become the extremely prominent air quality problem in urban areas of China (Deng et al., 2011; Huang et al., 2012; Ji et al., 2012; Cheng et al., 2013; Kang et al., 2013; Huang et., 2014; Zhang et al., 2014; Xie et al., 2016a; 2016c; Zhu et al., 2017). Many studies tried to reveal the contribution of meteorology to the severe particle pollution episodes as well. Chuang et al. (2008) identified seven weather patterns for aerosol events from March 2002 to February 2005 in the Taipei basin, and suggested that weather systems and the associated terrain blocking played important roles in the $PM_{2.5}$ accumulation during events days. Niu et al. (2010) revealed the potential impacts of weakening of the Eastern Asian monsoon circulation and increasing aerosol loading on the increase of wintertime fog in China. Zhao et al. (2013) analyzed a regional haze episode in the North China Plain from 16 to 19 January 2010, and pointed out that the strong temperature inversion, weak surface wind speed and descending air motions in the boundary layer were responsible for the accumulation of pollutants in a shallow layer and produced high pollutant concentrations within the source region. Zheng et al. (2015a) found that the favorable atmospheric circulation conditions are responsible for the severe winter haze over northeastern China. Li et al. (2016) pointed out that the fog-haze days over central and eastern China shows a clear feature of inter-annul variation, and the strong (weak) East Asian winter monsoon may result in less (more) fog-haze days across the region.

Located in the southeast coastal area of East China, the Yangtze River Delta (YRD) region is one of the most developed urban economic circles in the world, generally includes Shanghai, Jiangsu Province and Zhejiang Province, and occupies over 20% of China's total gross domestic product (GDP) (Shu et al., 2016; Xie et al., 2016a; 2017). In recent years, like other megacity clusters in China, such as the Beijing-Tianjin-Hebei (BTH) region (He et al., 2001; Chan and Yao, 2008; Ji et al., 2012; Zhang et al., 2012; 2014; Zhao et al., 2013; Zheng et al., 2015a) and the Pearl River Delta (PRD) region (Ho et al., 2003; Chan and Yao, 2008; Xie et al., 2016c; Zhu et al., 2017), YRD also has been suffering severe air pollution problems brought by accelerated population, urban expansion, and industrialization (Chan and Yao, 2008; Fu et al., 2008; 2010; 2014; Deng et al., 2011; Li et al., 2011; Huang et al., 2012; Kang et al., 2013; Wang et al., 2013; 2014; 2015; Xie et al., 2014; 2016a, 2016b, 2017; Feng et al., 2015; Zheng et al., 2015b; Shu et al., 2016; Xu et al., 2016; Ming et al., 2017). Especially, the severe particle pollution episodes are widely recognized as one of the major air pollution issues in YRD (Fu et al., 2008; 2010; Deng et al., 2011; Huang et al., 2012; Kang et al., 2013; Kong et al., 2013; Wang et al., 2013; 2014; 2015; Fu et al., 2014; Feng et al., 2015; Zheng et al., 2015b; Xu et al., 2016; Ming et al., 2017). Thus, a great deal of researches have been conducted to figure out the contamination status (Fu et al., 2010; Kang et al., 2013; Wang et al., 2013; 2015; Feng et al., 2015; Ming et al., 2017), possible source (Fu et al., 2010; 2014; Kong et al., 2013; Wang et al., 2013; 2014; Xu et al., 2016), or causes and features (Fu et al., 2008; 2010; Huang et al., 2012; Wang et al., 2015; Zheng et al., 2015a) of these episodes. However, among these studies, the work trying to figure out how particle pollution in YRD is associated with synoptic weather patterns is still quite limited. Zheng et al. (2015b) once summarized the synoptic-scale atmospheric circulations influencing the distribution of particles over eastern China in autumn from 2001 to 2010. They found that there are six polluted weather types and three clean ones, and revealed that heavy pollution events particularly occur when the study areas are at the rear of the anticyclone. This study considers the influence in a region larger than YRD, only focuses the pollution in October, and is mainly on basis of satellite aerosol optical depth (AOD) data. Ground-based monitoring particle concentration data can better represent the status of particle pollution in the urban atmosphere of YRD. Thus, to better understand the relationship between the pollution in planetary boundary layer and the synoptic weather patterns over YRD, further study should be conducted based on the data at least over a year from the surface monitoring in YRD.

This work attempts to enhance the understanding of particle pollution in YRD, and provides the scientific knowledge for the association of regional severe particle pollution and synoptic weather patterns. Firstly, we analyze the spatial and temporal distribution of PM_{10} and $PM_{2.5}$ in

YRD from December 2013 to November 2014, aimed to illustrate the characteristics of particle pollution over the region. Secondly, synoptic weather classification is conducted to reveal the weather patterns related with heavy pollution. Finally, synthetic analysis of meteorological fields and backward trajectory calculation are used to further clarify the impact mechanism. In this paper, Section 2 describes the observed data, synoptic weather classification method and the trajectory model. Section 3 presents our main findings, including the detailed analysis of the characteristics of particle pollution in YRD, the synoptic weather patterns affecting the pollution, and the mechanism how weather systems impact the pollution. In the end, a brief summary is addressed in Section 4.

2. Data and methods

2.1 Observed data

The observed air quality data ($PM_{2.5}$ and PM_{10}) used in this study are from the National Environmental Monitoring Center (NEMC) of China. The in situ monitoring data for the hourly concentrations of AQI, $PM_{2.5}$, PM_{10}, CO, NO_2, SO_2 and O_3 can be acquired from the national air quality real-time publishing platform (http://106.37.208.233:20035). Sixteen cities are selected as the representative research objects to better reflect the status of particle pollution over the YRD region. They are Shanghai, Changzhou, Nanjing, Nantong, Suzhou, Taizhoushi, Wuxi, Yangzhou, Zhenjiang, Hangzhou, Huzhou, Jiaxing, Ningbo, Shaoxing, Taizhou, and Zhoushan. Here we rename Taizhou in Jiangsu Province as Taizhoushi to distinguish it from the city Taizhou in Zhejiang Province. Fig. 1 shows the location of the 16 cities over YRD. The hourly pollutant concentration for a city is calculated as the average of the pollutant concentrations from several national monitoring sites in that city, which can better characterize the pollution levels of the city. The sampling methods and the quality assurance and quality control (QA/QC) procedures at each site act in accordance with the Chinese national standard HJ/T193-2005 (State Environmental Protection Administration of China, 2006; Xie et al., 2016b). Furthermore, manual inspection is conducted in data processing, including the removal of the absent and the abnormal values (such as $PM_{2.5}$ higher than PM_{10}). The period of this study starts from December 2013 to November 2014. In the following analysis, winter refers to the period from December 2013 to February 2014. Accordingly, spring, summer and fall represent the period from March to May, June to August,

Atmos. Chem. Phys. Discuss., https://doi.org/10.5194/acp-2017-473
Manuscript under review for journal Atmos. Chem. Phys.
Discussion started: 2 June 2017

and September to November in 2014, respectively.

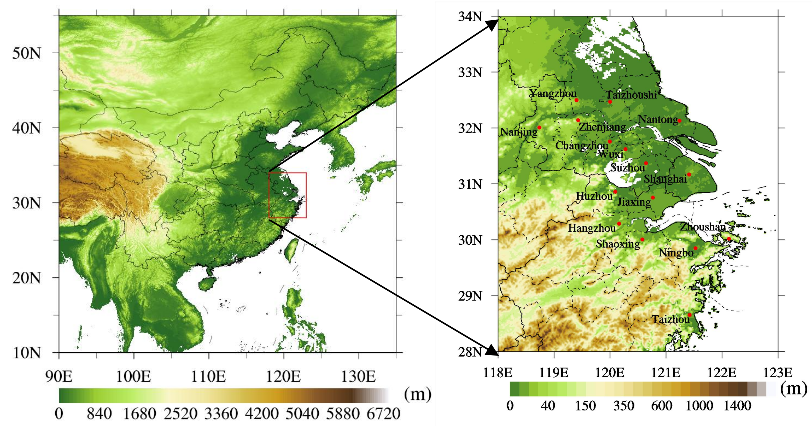

Figure 1. The location of YRD in China and the 16 typical cities over the YRD region, with the terrain elevations data. The terrain elevations data are obtained from the website (https://www.ngdc.noaa.gov/mgg/global/relief/ETOPO1/data/bedrock/cell_registered/).

2.2 Synoptic weather classification

Synoptic weather classification refers to the analysis of historical weather charts and characterization of weather systems. It has widespread applications in the weather forecast, and is more effective for the disastrous weather forecast due to its intense atmospheric circulation situation. With the gradual popularization of computer and greater sharing of data, synoptic weather classification has great practical value in many other research fields, for example, the field of analyzing the weather patterns related with air pollution (Mcgregor and Bamzelis, 1995; Zhang et al., 2012; Santurtún et al., 2015).

Methods of synoptic weather classification can be generally divided into the objective and the subjective methods (El-Kadi and Simithson, 1992). In this study, we apply the sums-of-squares technique, which is one of the objective classification methods and established in 1973 by Kirchhofer (Kirchhofer, 1973). The sums-of-squares technique can effectively categorize more than 90% of the analyzed weather maps, which is an improvement over the correlation techniques (Yarnal, 1984). The steps of applying this technique are threefold. Firstly, the daily pressure data at grid points are normalized as follows:

Atmos. Chem. Phys. Discuss., https://doi.org/10.5194/acp-2017-473
Manuscript under review for journal Atmos. Chem. Phys.
Discussion started: 2 June 2017

$$Z_i = \frac{(X_i - \overline{X})}{s} \quad (1)$$

where Z_i is the normalized value of the grid point i, X_i is the value at grid point i, $\overline{X}$ is the mean of the study domain, and s is the standard deviation. Data normalization removes the effects of pressure magnitude and improves the seasonal comparability of weather types. Secondly, each normalized grid is compared to all other grids on the basis of the Kirchhofer score (S) for each grid:

$$S = \sum_{i=1}^{N}(Z_{ai} - Z_{bi}) \quad (2)$$

where Z_{ai} is the normalized value in grid i on the day a, Z_{bi} is the normalized value in grid i on the day b, and N is the number of grid points. The Kirchhofer score (S) is calculated for each row (denoted as S_R), each column (S_C) and the entire study domain (S_T) to ensure the pattern similarity between any pair of patterns for all grid points. Finally, all days are separated into one of the identified synoptic weather patterns according to the three values and empirically derived thresholds. Thereinto, the values of S_R, S_C and S_T must be lower than their respective threshold values so that the patterns can be accepted as similar (Barry et al., 1981). For each daily grid, the lowest significant Kirchhofer score (S) is recorded with the associated key day denoting the synoptic type of the day. Remaining days are considered as 'unclassified'.

The dataset of meteorological field used in the sums-of-squares technique is from NCEP–DOE AMIP-II Reanalysis 2 data (Kanamitsu et al., 2002), which are collected at 00:00, 06:00, 12:00, and 18:00 UTC (universal time coordinated) (https://www.esrl.noaa.gov/psd/data/gridded/data.ncep.reanalysis2.pressure.html). The data have horizontal grids of 144×73, with a grid spacing of 2.5°. From the ground level to 10 hPa, there are 17 pressure levels in the vertical direction. The classification of synoptic weather maps is conducted by using the gridded data at the geopotential height of 850 hPa during the same time period when the air quality data are recorded. The domain of interest is centered over the YRD region, covering an area of 25-40° N in latitude and 110-128°E in longitude.

2.3 HYSPLIT model

Backward trajectories can be adopted to help understand transport paths and identify source regions of air masses (Shan et al., 2009). The Hybrid Single-Particle Lagrangian Integrated Trajectory (HYSPLIT) Model (Version 4) is developed by National Oceanic and Atmospheric Administration (NOAA) Air Resources Laboratory (ARL). It is one of the most extensively used atmospheric transport and dispersion models for the study of air parcel trajectories (Draxler and Rolph, 2013; Rolph, 2013; Stein et al., 2016), and has been well applied in complex transport, diffusion, chemical transformation and deposition processes simulations of atmospheric pollutants (Mcgowan and Clark, 2008; Wang et al., 2011; Huang et al., 2015; Xie et al., 2016b).

In this study, HYSPLIT is used to compute the air parcel backward trajectories, determine the source region of air masses, and establish the source-receptor relationships for each synoptic weather pattern. The 72-h backward trajectories are calculated and clustered. The ending point is set at 1500 m above sea level. The NCEP reanalysis data (http://ready.arl.noaa.gov/archives.php) are used to drive the backward trajectory calculation. The NCEP data contain 6-hourly basic meteorological fields on pressure surfaces with the spatial resolution of 2.5°. In this study, the data are also converted to hemispheric 144 by 73 polar stereographic grids, which is the same grid configuration as the dataset applied in synoptic weather classification. For each synoptic weather pattern, the terminus of the trajectories is considered to be located at the observation site in Nanjing (32°N, 118.8°E).

3. Results and discussion

3.1 Characteristics of particle pollution in the YRD region

3.1.1 Spatial distributions of particle pollution

With the development of modern industrialization and urbanization, the contrasts of atmospheric pollution levels between each city decrease gradually, and the heavy air pollution episodes tend to exhibit significant regional pollution characteristics. Fig. 2 respectively shows the spatial distributions of the annual mean concentrations of $PM_{2.5}$ (Fig. 2a) and PM_{10} (Fig. 2b) in the 16 typical cities over YRD from December 2013 to November 2014. The spatial distributions present the similar pattern as a whole. Taken together, the annual mean $PM_{2.5}$ and PM_{10} concentrations decrease progressively along the northwest-southeast direction, which means particle concentrations are comparatively high in the northwest inland areas and low in the southeast coastal areas. The pollution levels in most cities have a positive correlation with the

Atmos. Chem. Phys. Discuss., https://doi.org/10.5194/acp-2017-473
Manuscript under review for journal Atmos. Chem. Phys.
Discussion started: 2 June 2017

Atmospheric Chemistry and Physics Discussions

proximity from the city to the sea. The farther the city is from the sea, the higher the concentrations are. Thereinto, the maximum concentrations of $PM_{2.5}$ and PM_{10} occur in Nanjing, with the value of 79 and 130 $\mu g \cdot m^{-3}$, respectively. Given the previous researches on major climatic features in YRD, the southeast coastal area is dramatically affected by the land-sea breeze and marine air masses. The clean marine air masses are advantageous to the dilution and the diffusion of atmospheric pollutants, thus leading to lighter air pollution. Differently, in the inland region, the clustered cities and the industrial districts tend to emit more pollutants and thereby result in more accumulated air pollutants around cities.

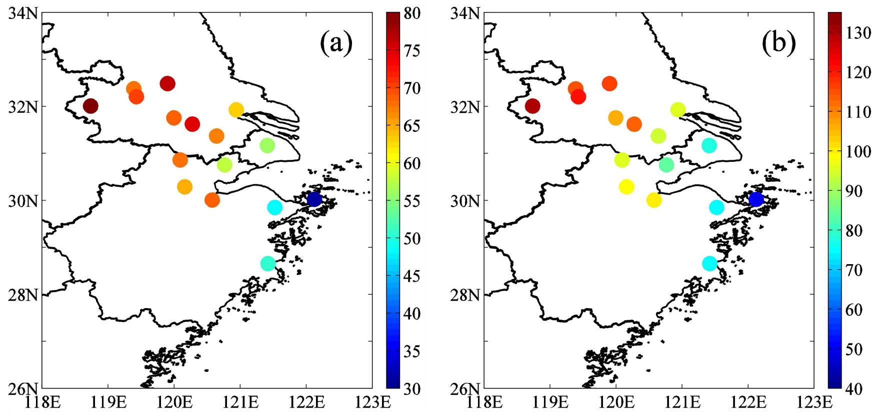

Figure 2. The spatial distributions of the annual mean concentrations of $PM_{2.5}$ (a) and PM_{10} (b) (unit: $\mu g \cdot m^{-3}$) over the YRD region from December 2013 to November 2014.

Fig. 3 illustrates the spatial distribution of the seasonal mean concentrations of $PM_{2.5}$ in 16 cities over the YRD region. The pattern in each season is similar to the annual mean pattern (Fig. 2a). The $PM_{2.5}$ pollution levels are much higher in inland cities, and decrease along the northwest-southeast direction. From the perspective of seasonal variation, $PM_{2.5}$ concentrations are highest in winter with the maximum value being up to 120 $\mu g \cdot m^{-3}$, decrease through the spring, and show the lowest values in summer and autumn. The difference between the $PM_{2.5}$ concentration in summer and that in autumn is relatively small, with the maximum value lower than 60 $\mu g \cdot m^{-3}$ and the minimum close to 20 $\mu g \cdot m^{-3}$.

Atmos. Chem. Phys. Discuss., https://doi.org/10.5194/acp-2017-473
Manuscript under review for journal Atmos. Chem. Phys.
Discussion started: 2 June 2017

Atmospheric Chemistry and Physics Discussions
Open Access

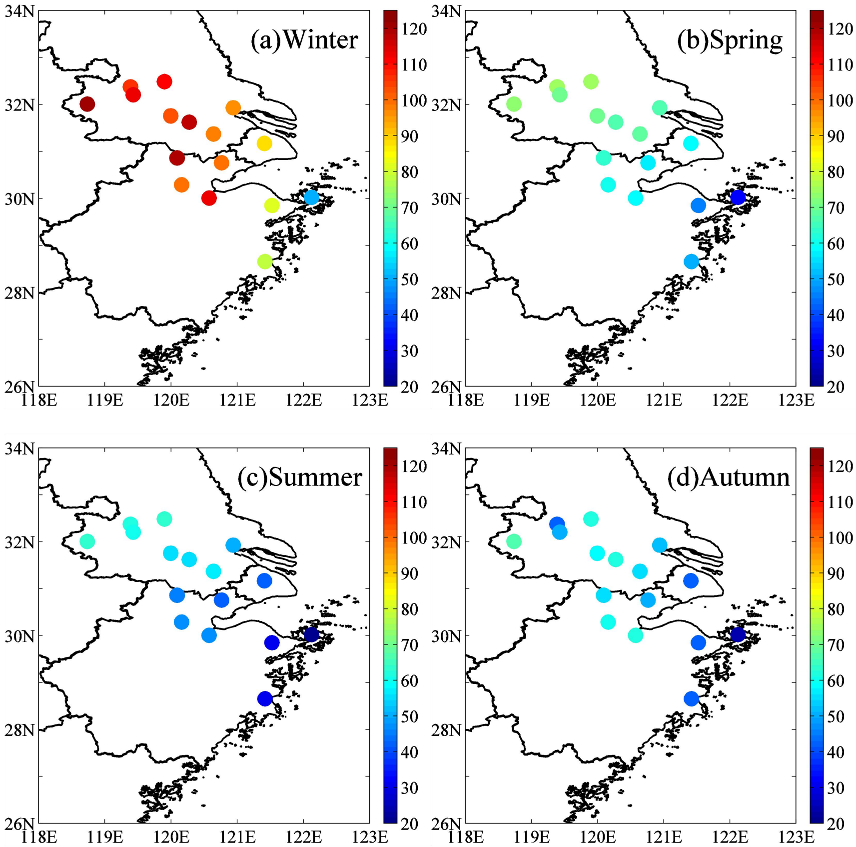

Figure 3. The spatial distribution of the seasonal mean $PM_{2.5}$ concentrations (unit: $\mu g \cdot m^{-3}$) over the YRD region: (a) winter, (b) spring, (c) summer, and (d) autumn.

Table 1 demonstrates the annual mean concentrations of $PM_{2.5}$ and PM_{10} in 16 cities over the YRD region. It shows that the concentrations in inland cities are relatively higher. The concentrations of $PM_{2.5}$ and PM_{10} in 8 cities of Jiangsu province are higher than 60 $\mu g \cdot m^{-3}$ and 80 $\mu g \cdot m^{-3}$, respectively. However, the concentrations in the cities located in the coastal area (such as Ningbo, Taizhou and Zhoushan) are comparatively lower. Only the air quality of Zhoushan meets the national standard, which may be attributed to the fact that it is located on the island where the air is more likely influenced by the clean marine air masses.

To reveal the important role of $PM_{2.5}$ in particle pollution, the ratios of $PM_{2.5}$ concentration to PM_{10} concentration ($PM_{2.5}/PM_{10}$) are calculated over YRD. As listed in Table 1, the maximum annual mean value of the $PM_{2.5}/PM_{10}$ ratio is 0.72 in Shanghai, followed by Huzhou and Suzhou

Atmos. Chem. Phys. Discuss., https://doi.org/10.5194/acp-2017-473
Manuscript under review for journal Atmos. Chem. Phys.
Discussion started: 2 June 2017

(with the value of 0.71), implying that $PM_{2.5}$ fraction is overwhelmingly dominant of the PM_{10} mass in these cities. The $PM_{2.5}/PM_{10}$ ratios in other cities are between 0.60 and 0.69, with the minimum value of 0.58 in Zhenjiang. These values are comparable to those in other cities like Beijing (He et al., 2001), Shanghai (Wang et al., 2013), Taiwan (Chen et al., 1999), and Hong Kong (Ho et al., 2003), suggesting that the formation of $PM_{2.5}$ from gases is the most importance source of particles in the cities of China. Table 1 also presents that the $PM_{2.5}/PM_{10}$ ratios in all cities show a distinct seasonal variation. It is remarkable that the values of $PM_{2.5}/PM_{10}$ in winter are much higher than those in other seasons, with the maximum value reaching 0.85 in Shanghai and followed by 0.82 in Suzhou. The highest concentrations of $PM_{2.5}$ usually occur in winter (Fig. 3a) and high values of $PM_{2.5}/PM_{10}$ ratio also appear in the same season (Table 1), suggesting that $PM_{2.5}$ poses a greater threat to human health in cold seasons that may be related to the heating activities. In summer, the values of $PM_{2.5}/PM_{10}$ in 16 cities the ratios are medium, with the mean value of 0.67. The lowest ratios usually occur in spring and autumn, with the mean ratios of all cities being 0.61 (spring) and 0.63 (autumn). The minimum value occurs in the autumn of Yangzhou with the value of 0.51, followed by 0.52 in the spring of Nanjing and the autumn of Zhenjiang. The above discussion about the spatial and temporal variations of $PM_{2.5}/PM_{10}$ ratios also implies that particles originate from various kinds of sources and are variedly emitted.

Table 1. Annual mean concentrations of $PM_{2.5}$ and PM_{10}, and the annual and seasonal mean values of $PM_{2.5}/PM_{10}$ ratio in 16 cities over the YRD region.

Cities		$PM_{2.5}$ ($\mu g \cdot m^{-3}$)	PM_{10} ($\mu g \cdot m^{-3}$)	$PM_{2.5}/PM_{10}$				
				Annual	Winter	Spring	Summer	Autumn
Shanghai		56	78	0.72	0.85	0.68	0.72	0.66
Jiangsu Province	Nanjing	79	130	0.61	0.64	0.52	0.70	0.60
	Changzhou	69	106	0.65	0.73	0.60	0.67	0.62
	Nantong	63	95	0.66	0.72	0.62	0.71	0.64
	Suzhou	67	94	0.71	0.82	0.68	0.71	0.67
	Taizhoushi	76	117	0.65	0.66	0.58	0.72	0.66
	Wuxi	75	114	0.66	0.73	0.59	0.67	0.62
	Yangzhou	68	114	0.60	0.69	0.58	0.59	0.51
	Zhenjiang	70	121	0.58	0.71	0.54	0.58	0.52
Zhejiang Province	Hangzhou	65	99	0.66	0.74	0.59	0.63	0.66
	Huzhou	68	96	0.71	0.78	0.66	0.68	0.69
	Jiaxing	58	84	0.69	0.75	0.65	0.68	0.69

Ningbo	48	75	0.64	0.69	0.62	0.63	0.62
Shaoxing	68	100	0.68	0.72	0.62	0.71	0.68
Taizhou	50	75	0.67	0.69	0.66	0.66	0.65
Zhoushan	31	50	0.63	0.66	0.62	0.66	0.55

3.1.2 Temporal variations of particle pollution

Fig. 4 shows the annual mean diurnal variation of $PM_{2.5}$ (Fig. 4a) and PM_{10} (Fig. 4b) in 16 cities over YRD. Obviously, the diurnal cycles of particle concentrations in most cities follow the similar pattern. The $PM_{2.5}$ concentrations maintain comparably high values from 0:00 to 8:00. From then on, coinciding with more vehicle emission in rush hours, the concentrations go up rapidly from 8:00 to 12:00. After reaching the peak, $PM_{2.5}$ concentrations decrease and keep the low values until the sunset. During the nighttime, the pollutants get accumulated until the midnight, which might be attributed to the more stable atmospheric stratification in the boundary layer. In comparison, there are two peaks in the diurnal cycles of PM_{10} concentration in several cities. The broad morning peak of PM_{10} concentrations is more evident from 8:00 to 12:00, and the evening one occurs around 20:00. Besides, the diurnal change of particle concentrations in the southeast coastal area like Zhoushan is much smaller. As discussed in Section 3.1.1, the difference might be related to its special geographic location, low pollution level and less emission of precursors.

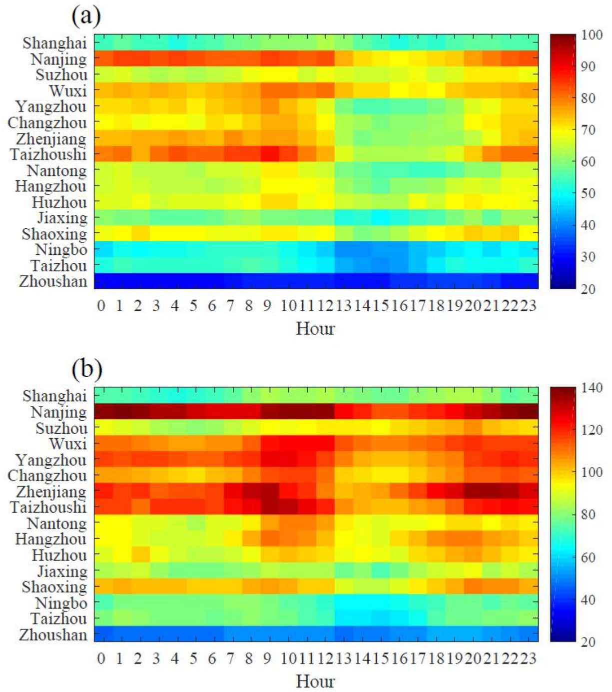

Figure 4. Diurnal variations of (a) $PM_{2.5}$ and (b) PM_{10} concentrations (unit: μg·m^{-3}) in 16 cities of the YRD region.

Fig. 5 demonstrates the monthly mean concentrations of $PM_{2.5}$ (Fig. 5a) and PM_{10} (Fig. 5b) in 16 cities of the YRD region. As illustrated in the figure, there are three peaks in the seasonal variations of particles over YRD. The three peaks occur in December, March, and May/June, which is more obvious in the monthly variation of PM_{10}. The causes result in the wintertime peak of particle concentrations can be explained by two factors. One is the enhanced pollutants emissions from residential heating. The other is the stable and poor meteorological conditions that limit the dilution and diffusion of atmospheric pollutants. For the peak appearing in March, the drivers may be associated with dust storms events in spring (Zhuang et al., 2001; Fu et al., 2010; 2014). As discussed in Section 3.1.1, the values of $PM_{2.5}/PM_{10}$ ratio in 16 cities are lowest in spring with the mean ratios of 0.61. High PM_{10} concentrations during this period further prove that dust storms bring more coarse dust particles. For the peak in May or June, it is probably caused by field burning of crop residue in rural areas of China, which is regarded as an important source of biomass burning (Yan et al., 2006; Yang et al., 2007; Zhu et al., 2012).

Atmos. Chem. Phys. Discuss., https://doi.org/10.5194/acp-2017-473
Manuscript under review for journal Atmos. Chem. Phys.
Discussion started: 2 June 2017

Atmospheric Chemistry and Physics
Discussions

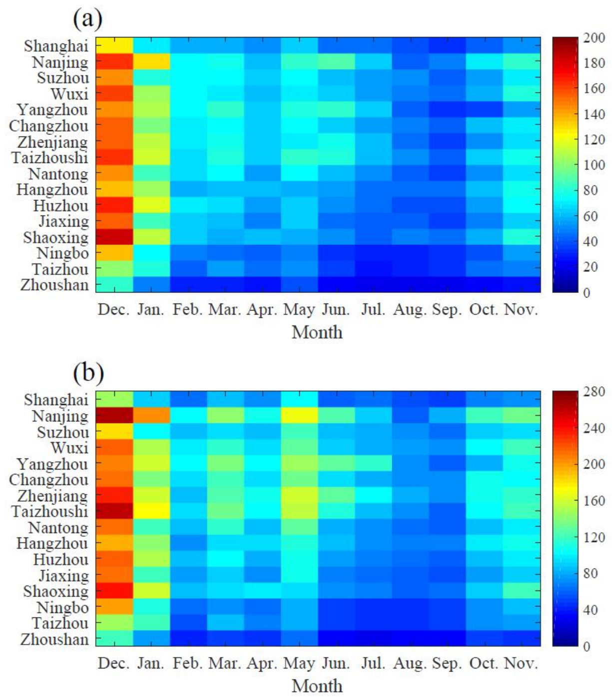

Figure 5. Monthly variations of (a) $PM_{2.5}$ and (b) PM_{10} concentrations (unit: $\mu g \cdot m^{-3}$) in 16 cities of the YRD region.

3.1.3 Regional severe particle pollution in YRD

According to the National Ambient Air Quality Standard (NAAQS) of China, the urban air quality needs to meet the second standard with the annual mean concentrations of $PM_{2.5}$ and PM_{10} lower than 35 $\mu g \cdot m^{-3}$ and 70 $\mu g \cdot m^{-3}$, respectively. In this study, when the daily mean $PM_{2.5}$ (PM_{10}) concentrations exceed the national air quality standard in most (8 or more) of the 16 YRD cities, we define that there is a large-scale regional $PM_{2.5}$ (PM_{10}) pollution. Consequently, from December 2013 to November 2014, 98 (46) days when the large-scale regional $PM_{2.5}$ (PM_{10}) pollution episode occurred are identified. That is, YRD suffered from the regional $PM_{2.5}$ (PM_{10}) pollution in nearly 28.0% (13.1%) days of the year.

Table 2 shows the typical regional severe particle pollution episodes (no less than 3 days) in YRD from December 2013 to November 2014. As illustrated in the table, there are dozens of continuous large-scale particle pollution episodes. For example, $PM_{2.5}$ concentrations exceeded the national standard in 16 cities from December 1 to 5 in 2013, and there were more than 14 cities facing the PM_{10} pollution at the same time. From May 26 to 30 in 2014, serious $PM_{2.5}$ and

Atmos. Chem. Phys. Discuss., https://doi.org/10.5194/acp-2017-473
Manuscript under review for journal Atmos. Chem. Phys.
Discussion started: 2 June 2017

PM_{10} pollution were found in more than 10 cities. It seems that high $PM_{2.5}$ level pollution episodes are remarkably associated with high PM_{10} level pollution episodes. Moreover, the regional $PM_{2.5}$ pollution episodes occurred much more frequently than the PM_{10} pollution episodes. It might be owing to the fact that fine particles dominate the composition of particles in YRD (as discussed in Section 3.1.2).

Table 2. The typical regional severe particle pollution episodes (no less than 3 days) in YRD from December 2013 to November 2014.

Episodes of $PM_{2.5}$ pollution	Episodes of PM_{10} pollution
1-6 Dec.	1-6 Dec.
11-15 Dec.	12-15 Dec.
24-26 Dec.	24-26 Dec.
28 Dec. - 6 Jan.	29 Dec. - 5 Jan.
15-20 Jan.	17-20 Dec.
30 Jan. - 2 Feb.	26-30 May
20-24 Feb.	
16-18 Mar.	
8-10 Apr.	
20-22 May	
26-30 May	
5-7 Jun.	
28 Jun. - 1 Jul.	
10-12 Nov.	

3.2 Synoptic weather classification

To examine the relationship between the regional severe particle pollution in YRD and the weather situations, the synoptic weather classification is carried out from December 2013 to November 2014 in this work. Follow the method described in Section 2.2, we conduct the classification of synoptic weather pattern by using the dataset of geopotential height at 850 hPa collected from NCEP gridded data. As shown in Table 3, five weather patterns are identified, including the East Asian trough rear pattern (Pattern 1), the depression inverted trough pattern (Pattern 2), the transversal trough pattern (Pattern 3), the high-pressure controlled pattern (Pattern 4), and the northeast cold vortex pattern (Pattern 5). The unknown type is defined as the unclassified pattern. During the study period, weather situation on 95.6% of the days is classified as one of the five typical synoptic weather patterns.

Atmos. Chem. Phys. Discuss., https://doi.org/10.5194/acp-2017-473
Manuscript under review for journal Atmos. Chem. Phys.
Discussion started: 2 June 2017

Table 3 lists the typical date, the number of days, and seasonal occurrence frequencies of each synoptic weather pattern. As demonstrated in the table, Pattern 1 is the dominant weather pattern in YRD, which accounts for 47.6% of all days of the year (from December 2013 to November 2014). The occurrence frequencies of Pattern 2 and 3 are 20.0% and 18.1%, respectively. Pattern 4 and 5 are identified on the fewest number of days, with the occurrence frequencies of 4.1% and 5.8%, respectively.

Table 3 also shows the seasonal occurrence frequencies of each pattern from December 2013 to November 2014. Obviously, they are distinctly different. Pattern 1 tends to occur in winter with the frequency of 30.5%, followed by spring (25.9%), summer (21.8%) and autumn (21.8%). Pattern 2 is the most popular weather pattern in summer with the occurrence frequency of 37.0%, followed by spring (30.1%), autumn (21.9%) and winter (11.0%). As for Pattern 3, the seasonal frequencies are in the order of winter (36.4%), spring (27.3%), autumn (19.7%) and summer (16.7%). For Pattern 4 and Pattern 5, they are both most likely to take place in autumn, with the occurrence frequencies being 53.3% and 42.9%, respectively. The occurrence frequencies of Pattern 4 and Pattern 5 in other seasons account for nearly 50%.

Table 3. The typical date, the number of days, and the seasonal occurrence frequencies of each synoptic weather pattern.

Synoptic weather patterns	Typical date	Number of days	Occurrence frequency (%)			
			Spring	Summer	Autumn	Winter
East Asian trough rear pattern (Pattern 1)	2014-05-12	174 (47.7%)	25.9	21.8	21.8	30.5
Depression inverted trough pattern (Pattern 2)	2014-05-09	73 (20.0%)	30.1	37.0	21.9	11.0
Transversal trough pattern (Pattern 3)	2014-02-18	66 (18.1%)	27.3	16.7	19.7	36.4
High-pressure controlled pattern (Pattern 4)	2014-10-07	15 (4.1%)	13.3	26.7	53.3	6.7
Northeast cold vortex pattern (Pattern 5)	2014-09-14	21 (5.8%)	19.0	23.8	42.9	14.3
Unclassified pattern	—	16 (4.4%)	—	—	—	—

3.3 Effects of synoptic weather patterns on particle pollution

3.3.1 Relationship between synoptic weather pattern and particle pollution

To figure out the relationship between synoptic weather pattern and particle pollution, the

Atmos. Chem. Phys. Discuss., https://doi.org/10.5194/acp-2017-473
Manuscript under review for journal Atmos. Chem. Phys.
Discussion started: 2 June 2017

occurrence frequencies of the five typical synoptic patterns during the regional severe particle pollution episodes are calculated. As shown in Table 4, during the regional $PM_{2.5}$ (PM_{10}) pollution episode days, Pattern 1 is the dominant synoptic weather pattern, with the occurrence frequency of 70.4% (78.3%). For $PM_{2.5}$ pollution, Pattern 2 and Pattern 3 both occur for 14.3% of the days. For PM_{10} pollution, Pattern 2 (6.5%) appears less frequently than Pattern 3 (15.2%). The occurrence frequencies of Pattern 4 and Pattern 5 are less than 1%, and can almost be ignored on that account.

According to Table 3 and Table 4, the occurrence frequency of Pattern 1 during the regional particle pollution episodes is obviously higher than its occurrence in the whole year. In contrast, the occurrences of Pattern 2 and Pattern 3 during the regional particle pollution episodes are less frequently than those throughout the year. Moreover, Pattern 4 and Pattern 5 appear far less frequently during the regional particle pollution episodes than their appearance within a year. To sum up, it suggests that the weather situation of Pattern 1 is more beneficial for the formation of large-scale regional particle pollution in YRD.

Table 4. The occurrence frequencies of synoptic weather patterns during the regional severe $PM_{2.5}$ and PM_{10} pollution episodes

Synoptic weather patterns	$PM_{2.5}$		PM_{10}	
	Number of days	Frequency (%)	Number of days	Frequency (%)
Pattern 1	69	70.4	36	78.3
Pattern 2	14	14.3	3	6.5
Pattern 3	14	14.3	7	15.2
Pattern 4	0	0%	0	0
Pattern 5	1	1.0	0	0

3.3.2 The impact mechanism of synoptic weather patterns on heavy particle pollution

Fig. 6 to 10 present the meteorological fields and the backward trajectories under the weather situations of the five synoptic weather patterns. The first graphs of Fig. 6 to 10, which are identified as a, illustrate the 850 hPa geopotential height field and wind field on the typical date of each pattern. The highlighted red boxes point out the essential area (YRD) that we focus on. The second graphs identified as b demonstrate the height-latitude cross-sections of vertical velocity in the latitude (25-40°N), which is averaged from 110-128°E in the longitude. The bold black lines show the latitude range of 16 cities (28.6-32.5°N) over YRD. The positive wind speeds (10^2 Pa s^{-1}) indicate that there are vertical downward atmospheric motions, while the negative wind speeds represent the upward motion. Besides, it is well known that the atmospheric pollutant transport trajectories are deeply affected by synoptic systems. As shown in the third graphs marked with c in Fig. 6 to 10, to reveal how the typical synoptic weather patterns influence the distribution of particles in YRD, the 72-h backward trajectories are calculated and then clustered. Given that Nanjing is the most polluted among the 16 cities in YRD as described in Section 3.1, the observational site in Nanjing (32°N, 118.8°E) is chosen for the terminus of the trajectories for each synoptic weather pattern.

As illustrated in Fig. 6a, Pattern 1 usually occurs when northeastern China is entirely affected by the Siberian high. East Asian major trough appears along the eastern coastline of China, and it is nearly close and parallel to the right edge of the study domain (shown by the red box). At this time, the YRD region is located at the rear of the East Asian major trough and the front edge of the ridge. The strong horizontal northwest wind in the front of the East Asia major trough can transport the pollutants from the Beijing-Tianjin-Hebei (BTH) region to YRD. At the same time, a weak low-pressure center appears in central China. In the south of the low-pressure center, the southwest wind can also transport the pollutants from the Sichuan Basin to YRD. The confluence of air flows may contribute to the accumulation of pollutants in YRD. The above discussion can be proved by the 72-h backward trajectories displayed in Fig. 6c. When YRD is under the control of Pattern 1, the air masses are mainly from the north of China (44%), followed by the Sichuan Basin (36%) and the north of YRD (19%). It suggests that the particle pollution is remarkably affected by the polluted air masses from BTH and Cheng-Yu agglomeration.

In the vertical section (Fig. 6b), the upward air flows dominate in the south of 32°N, while the downward air flows prevail in the north of 32°N. The largest ascending velocity ($< -15\times10^{-2}$ Pa s^{-1}) and subsiding velocity ($> 24\times10^{-2}$ Pa s^{-1}) both appear at the altitude of 500 hPa. They respectively occur in the latitude of 27.5°N and 37.5°N. It is convinced that there is a large-scale vertical atmospheric circulation above the YRD cities. Particularly, weak upward motion dominates below the altitude of 925 hPa. That means that local pollutants are transported upward and then back to the YRD cities by the strong outward downdrafts in the higher latitude. The strong horizontal northwest wind hinders the vertical transport. Overall, this weather situation is disadvantageous to the diffusion of atmospheric pollutants. This result is consistent with the finding of Zheng et al (2015b).

Atmos. Chem. Phys. Discuss., https://doi.org/10.5194/acp-2017-473
Manuscript under review for journal Atmos. Chem. Phys.
Discussion started: 2 June 2017

Atmospheric Chemistry and Physics
Open Access
Discussions

Pattern 1

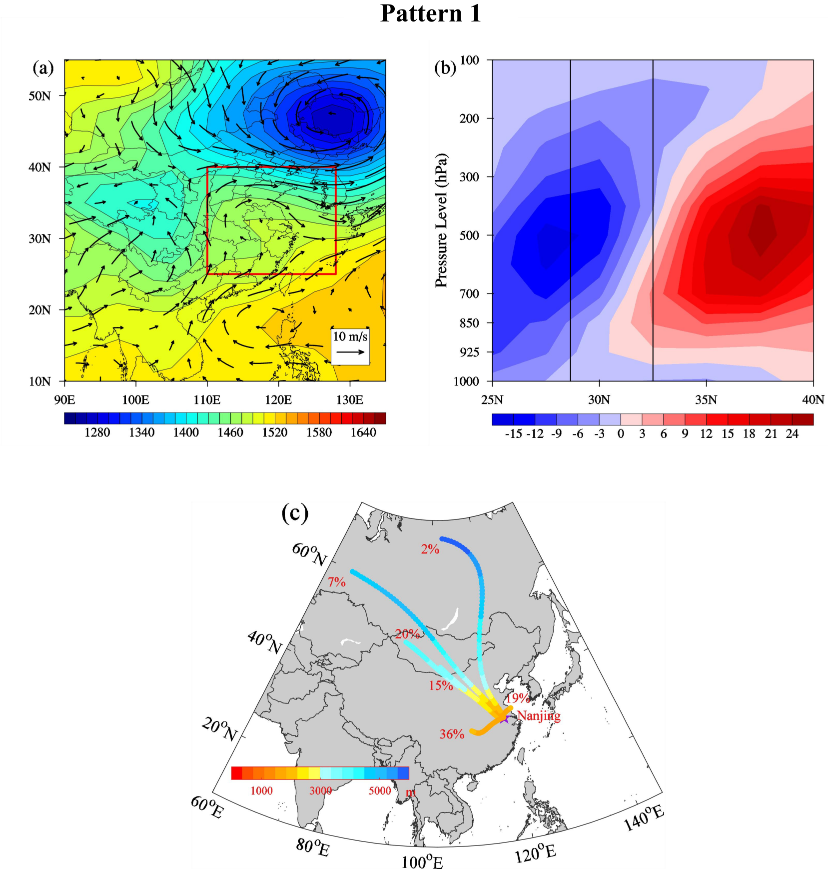

Figure 6. East Asia major trough rear pattern (Pattern 1). (a) 850 hPa geopotential height field and wind field, (b) height-latitude cross-sections of vertical velocity (unit: 10^{-2} Pa/s) averaged from longitude of 110-128°E. The black rectangular region represents the 16 cities in YRD (28.6-32.5°N), and (c) 72-h backward trajectory ending at the height of 1500 m. The purple marker indicates the location of Nanjing (32°N, 118.8°E).

As for Pattern 2, two low-pressure centers are centered in the central China and the north of Inner Mongolia region, the East China Sea is influenced by a high-pressure system, and a depression inverted trough extends and covers the YRD region in latitude (Fig. 7a). Consequently, in YRD, the strong southwest air flows from southern China meet with the southeast air flows from the East China Sea. After the convergence of air masses, they jointly transport pollutants northwestward. Fig. 7c also illustrates these air pollutant transport paths. For the days when Pattern 2 dominates, about 42% of the air masses are from the southwest and the south of China, and 15% are from the East China Sea. Besides, there are nearly 43% originating from the local

Atmos. Chem. Phys. Discuss., https://doi.org/10.5194/acp-2017-473
Manuscript under review for journal Atmos. Chem. Phys.
Discussion started: 2 June 2017

Atmospheric Chemistry and Physics
Discussions
Open Access

sources of YRD, which may be related with the short-range air masses transport. The air masses from the East China Sea are very important, because the clean marine air masses may dilute the particle concentrations in YRD. For the vertical structure (Fig. 7c), the upward air flows dominate in the south of 34ºN except for weak downward motion between 30-33ºN below the 850 hPa layer. The largest updrafts zone (< -15×10^{-2} Pa s^{-1}) appears in the north of 28ºN and between the altitude of 700 hPa and 500 hPa. Different from Pattern 1, there is weaker descending motion above the 500 hPa layer and stronger ascending motion below that level. This difference suggests that pollutants in YRD are horizontally transported northwestward to higher latitude, and vertically transport upward to high atmospheric levels. Thus, though Pattern 2 may cause the regional particle pollution in YRD, it can also benefit the diffusion of pollutants to some extent.

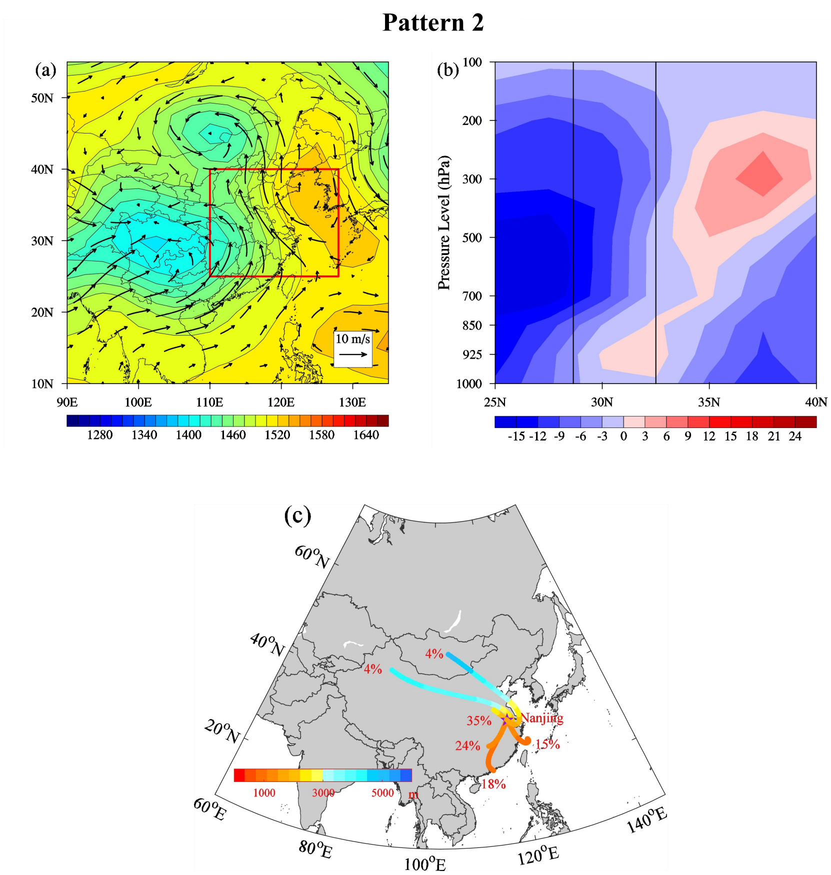

Figure 7. As in Fig. 6 but for depression inverted trough pattern (Pattern 2).

For Pattern 3, it tends to occur in winter (36.4%, as displayed in Table 3). Under this circumstance, the Qinghai-Tibet Plateau is usually regarded as a cold source. A strong cold high-pressure system is formed in the lower layer of the plateau, accompanied by an anti-cyclonic circulation (Fig. 8a). Meanwhile, the northeastern China is under the steering influence of the high-pressure ridge. A transversal trough covers the YRD region, and its axis orienting from the northeastern sea areas to southwest inland areas. Affected by the strong northeast wind from the Yellow Sea, the polluted northwest air flows in the north of transversal trough are slowed down. The above discussion is further proved by the results from back trajectory calculations. As suggested in Fig. 8c, most air masses in clusters are from the Loess Plateau, with the percentage of 31%. The transport path of this cluster is relatively short, which might be attributed to the weakened northwest wind. The long-range transport of air masses from remote Mongolia also accounts for 22% of all trajectories. Besides, the local transport of air masses from the southeast coastal area in YRD accounts for 26%, which is associated with the northeast air flows. The marine air masses cluster originates from western Pacific via the Yellow Sea accounts for 4%. They both bring the clean marine air masses to YRD, which is somewhat beneficial to the mitigation of particle pollution in YRD. For the vertical structure (Fig. 8b), the distribution of vertical velocity below the altitude of 300 hPa is similar to that of Pattern 1, whereas the vertical wind is slower for the weather systems in Pattern 3. Thus, influenced by the downdrafts in higher latitudes and horizontal northeast air flows, more clean marine air masses may be transported to YRD. In all, Pattern 3 may cause particle pollution in YRD when the north polluted air masses are transported in, but it is also conducive to the diffusion of pollutants because of the clean marine air masses.

Atmos. Chem. Phys. Discuss., https://doi.org/10.5194/acp-2017-473
Manuscript under review for journal Atmos. Chem. Phys.
Discussion started: 2 June 2017

Atmospheric Chemistry and Physics Discussions
Open Access

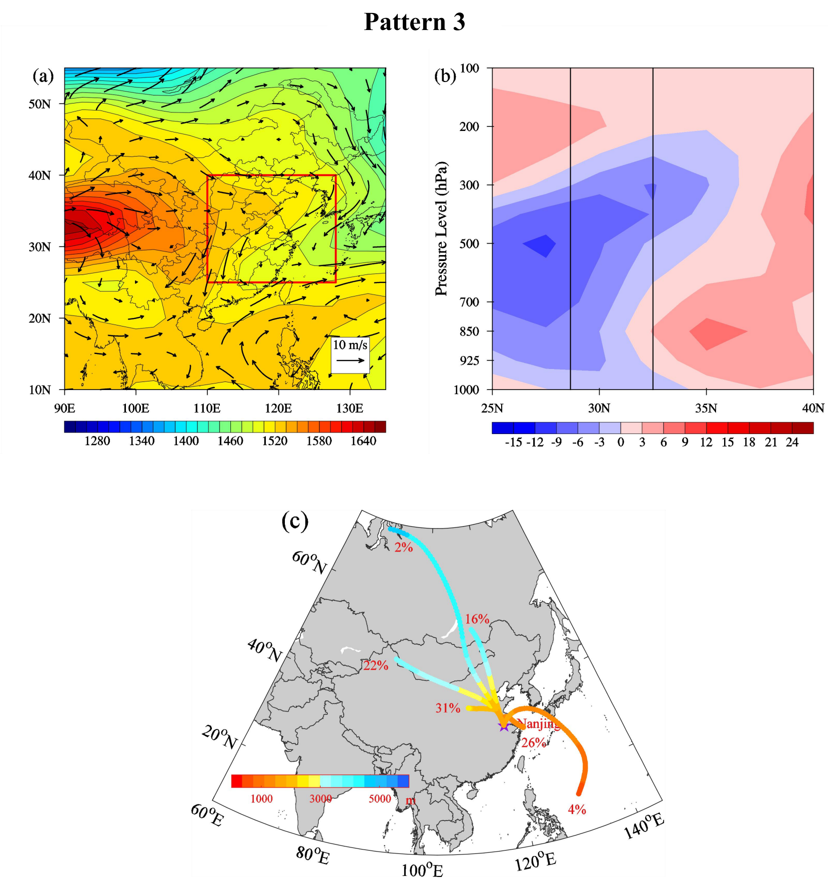

Figure 8. As in Fig. 6 but for transversal trough pattern (Pattern 3).

With respect to Pattern 4, the study domain is totally under the control of a high-pressure system (Fig. 9a). The anti-cyclonic circulation prevails over YRD and horizontally brings the clean marine air masses to the land. Accordingly, influenced by the high-pressure system, the downward atmospheric motion dominates in the vertical direction obviously (Fig. 9b). The weak updrafts near the surface may be related to the regional thermodynamic circulation. As shown in Fig. 9c, the cluster with the largest frequency of 32% stands for the local transport of air masses from southern adjacent areas in YRD. Additionally, the air masses from North China via Bohai Bay (25%), from Japan via the Yellow Sea (23%), and from the Philippines via the East China Sea (5%) are also representative. These clusters passing over the ocean areas totally account for more than 50% of all trajectories. Therefore, under this weather situation, it is confirmed that the dilution effects of clean marine air masses play great roles in the particle pollution over YRD.

Atmos. Chem. Phys. Discuss., https://doi.org/10.5194/acp-2017-473
Manuscript under review for journal Atmos. Chem. Phys.
Discussion started: 2 June 2017

Pattern 4

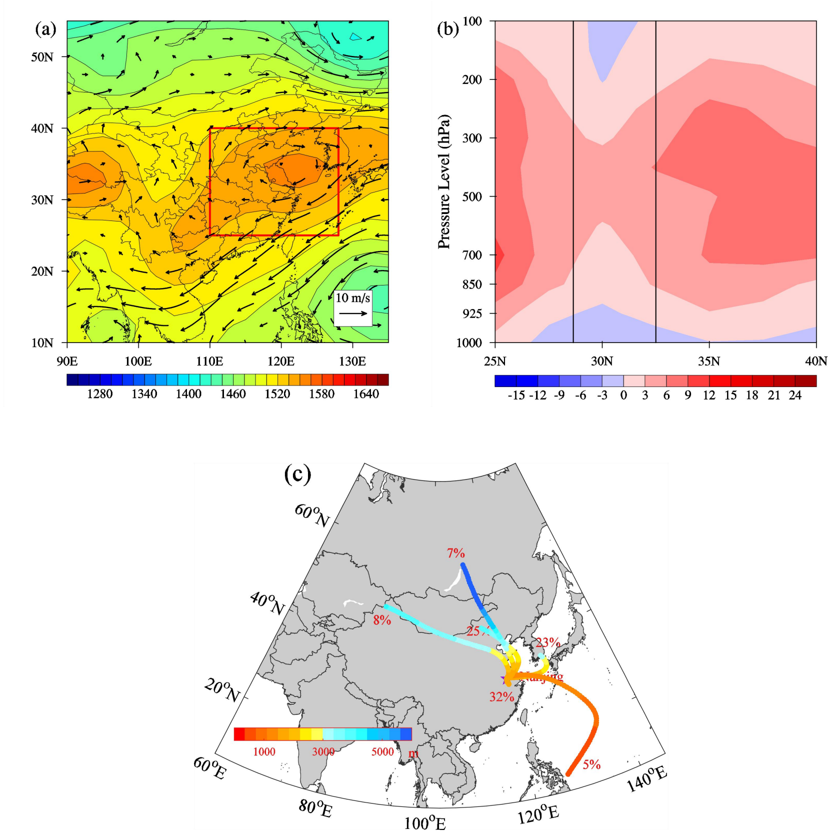

Figure 9. As in Fig. 6 but for high-pressure controlled pattern (Pattern 4).

Finally, Pattern 5 features the most complex circulation situation (Fig. 10a). The northeastern China is controlled by a cold eddy system. The central China is impacted by a high-pressure ridge. A strong tropical low-pressure system is located around Luzon. At this time, YRD is located in the south of the central high-pressure system and north of the strong tropical low-pressure system. The horizontal southeast wind prevails and carries clean marine air masses from the East China Sea to YRD. At the same time, upward air flows are dominant and comparatively weak (>-3×10^{-2} Pa s^{-1}) in the lower troposphere (Fig. 10b). According to Fig. 10c, the cluster with the largest frequency of 45% consists of the wet air parcels from Japan via the Yellow Sea. Only 5% of the trajectories originates from the Philippines and pass over the East China Sea. On the whole, the weather systems in Pattern 4 and 5 are both mainly influenced by the clean marine air masses, and largely beneficial to the diffusion of the pollutants.

Atmos. Chem. Phys. Discuss., https://doi.org/10.5194/acp-2017-473
Manuscript under review for journal Atmos. Chem. Phys.
Discussion started: 2 June 2017

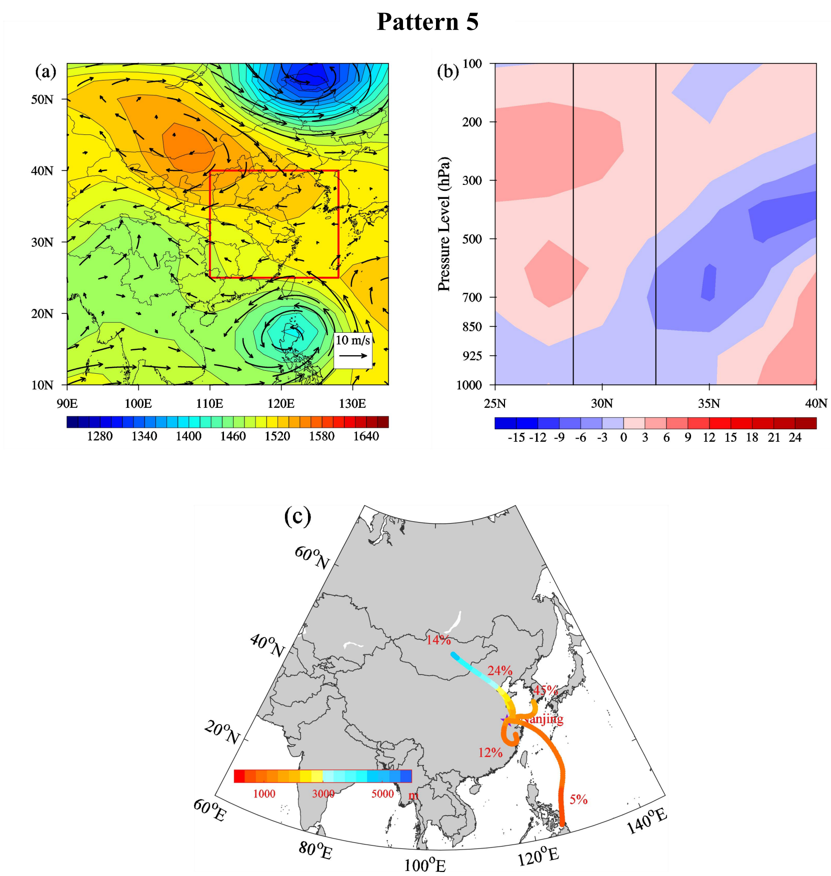

Figure 10. As in Fig. 6 but for northeast cold vortex pattern (Pattern 5).

To sum up, under the influence of weather system of Pattern 1, the particle pollution in YRD is largely affected by the transport of pollutants from the south and north inland regions of China. This weather situation is extremely not favorable to the diffusion of air pollutants, and responsible for the most large-scale particle pollution episodes over YRD. As for Pattern 2 and Pattern 3, the polluted air masses mainly travel from inland areas, and synchronously meet with the clean marine air masses in YRD. To some extent, this weather situation is helpful to the mitigation of particle pollution in YRD. With respect to Pattern 4 and Pattern 5, YRD is directly influenced by the air flows traveling from the ocean areas, and has little chance of being polluted. It suggests that the clean marine air masses have great dilution impacts on the particle pollution over YRD.

4. Conclusions

In this study, the spatial and temporal distribution of particle pollution in 16 YRD cities are characterized from December 2013 to November 2014. Meanwhile, the synoptic weather classification is conducted to identify the dominant weather patterns over YRD. The meteorological fields and 72-h backward trajectories are analyzed to reveal the potential impacts of weather systems on the regional severe particle pollution.

From the observational records, it is shown that the concentrations of $PM_{2.5}$ and PM_{10} decrease progressively along the northwest-southeast direction. The pollution levels are comparatively high in the Jiangsu Province and much lower in the southeast coastal area (Ningbo, Taizhou and Zhoushan). The highest particle concentration occurs in Nanjing, with the concentrations of $PM_{2.5}$ and PM_{10} being 79 $\mu g \cdot m^{-3}$ and 130 $\mu g \cdot m^{-3}$, respectively. The $PM_{2.5}/PM_{10}$ ratios are high in YRD, especially in winter. The seasonal mean $PM_{2.5}/PM_{10}$ ratios are 0.73 (winter), 0.61 (spring), 0.67 (summer) and 0.63 (autumn), respectively. These high $PM_{2.5}/PM_{10}$ ratios suggest that the $PM_{2.5}$ fraction is extraordinarily dominant in the PM_{10} mass in YRD. The diurnal cycles of particle concentrations in most cities follow the same pattern, with a morning peak from 8:00 to 12:00. There are three peaks in seasonal variations (December, March, and May or June). The wintertime peak is closely related to the enhanced emissions in the heating season and poor meteorological conditions. YRD suffered from the $PM_{2.5}$ (PM_{10}) pollution in nearly 28.0% (13.1%) days of the year. The continuous large-scale regional $PM_{2.5}$ pollution episodes occur much more frequently than the PM_{10} pollution episodes.

Based on the sums-of-squares technique, five typical synoptic weather patterns are objectively classified in YRD, including the East Asia major trough rear pattern (47.7%), the depression inverted trough pattern (20.0%), the transversal trough pattern (18.1%), the high-pressure controlled pattern (4.1%) and the northeast cold vortex pattern (5.8%). When YRD is located at the rear of the East Asian major trough (Pattern 1), it is primarily influenced by the polluted air masses traveling from southern and northern inland regions. The analysis of meteorological field also indicates that the strong horizontal northwest wind hinders the vertical outward transport of pollutants. Thus, this weather situation is extremely unfavorable for the diffusion of the pollutants, and contributes most to the occurrence of large-scale regional $PM_{2.5}$ (70.4%) and PM_{10} (78.3%) pollution episodes in YRD. In contrast, under the weather system of other synoptic patterns, especially Pattern 4 and 5, the clean marine air masses play crucial roles in the mitigation of pollution over YRD. Under these weather patterns, YRD has much less chance of being polluted.

In summary, the above results reveal that the particle pollution in China is no longer a thorny issue over a single city, but over a regional scale. This study can enhance the understanding of features of particle pollution in East Asia. Meanwhile, it also confirmed that large-scale synoptic weather systems have great impacts on region particle pollution episodes. Therefore, the establishment of the potential links between different levels of particle pollution and predominant synoptic patterns can provide an insightful view on formulating pollution control and mitigation strategies.

Acknowledgments

This work was supported by the National Natural Science Foundation of China (41475122, 91544230, 91537102, 41621005), the National Key Research and Development Program of China (2016YFC0203303, 2016YFC0208504, 2016YFA0602104), and open research fund of Chongqing Meteorological Bureau (KFJJ-201607). The authors would like to thank the anonymous reviewers for their constructive and precious comments on this manuscript.

References

Barry, R. G., Kiladis, G., and Bradley, R. S.: Synoptic climatology of the Western United States in relation to climatic fluctuations during the twentieth century, International Journal of Climatology, 1, 97-113, 1981.

Brook, R. D., Rajagopalan, S., Pope, C. A., Brook, J. R., Bhatnagar, A., Diez-Roux, A. V., Holguin, F., Hong, Y., Luepker, R. V., and Mittleman, M. A.: Particulate matter air pollution and cardiovascular disease, Circulation, 121, 2331-2378, 2010.

Buchanan, C., Beverland, I. J., and Heal, M. R.: The influence of weather-type and long-range transport on airborne particle concentrations in Edinburgh, UK, Atmospheric Environment, 36, 5343-5354, 2002.

Chan, C. K., and Yao, X.: Air pollution in mega cities in China, Atmospheric environment, 42, 1-42, 2008.

Chen, M. L., Mao, I. F., and Lin, I. K.: The PM 2.5 and PM 10 particles in urban areas of Taiwan, Science of the Total Environment, 226, 227-235, 1999.

Cheng, Z., Jiang, J., Fajardo, O., Wang, S., and Hao, J.: Characteristics and health impacts of particulate matter pollution in China (2001–2011), Atmospheric Environment, 65, 186-194, 2013.

Chuang, M.-T., Chiang, P.-C., Chan, C.-C., Wang, C.-F., Chang, E., and Lee, C.-T.: The effects of synoptical weather pattern and complex terrain on the formation of aerosol events in the

Greater Taipei area, Science of the total environment, 399, 128-146, 2008.
Deng, J. J., Wang, T. J., Jiang, Z. Q., Xie, M., Zhang, R. J., Huang, X. X., Zhu, J. L.: Characterization of visibility and its affecting factors over Nanjing, China. Atmos Res, 101, 681-691, 2011.
Draxler, R., and Rolph, G.: HYSPLIT (HYbrid Single-Particle Lagrangian Integrated Trajectory), NOAA Air Resources Laboratory, College Park, MD, Model access via NOAA ARL READY Website, 2013.
El-Kadi, A. K. A., and Smithson, P. A.: Atmospheric classifications and synoptic climatology, Progress in Physical Geography, 16, 432-455, 1992.
Feng, J., Hu, J., Xu, B., Hu, X., Sun, P., Han, W., Gu, Z., Yu, X., and Wu, M.: Characteristics and seasonal variation of organic matter in PM 2.5 at a regional background site of the Yangtze River Delta region, China, Atmospheric Environment, 123, 288-297, 2015.
Flocas, H., Kelessis, A., Helmis, C., Petrakakis, M., Zoumakis, M., and Pappas, K.: Synoptic and local scale atmospheric circulation associated with air pollution episodes in an urban Mediterranean area, Theoretical and Applied Climatology, 95, 265-277, 2009.
Fu, Q., Zhuang, G., Wang, J., Xu, C., Huang, K., Li, J., Hou, B., Lu, T., and Streets, D. G.: Mechanism of formation of the heaviest pollution episode ever recorded in the Yangtze River Delta, China, Atmospheric Environment, 42, 2023-2036, 2008.
Fu, Q., Zhuang, G., Li, J., Huang, K., Wang, Q., Zhang, R., Fu, J., Lu, T., Chen, M., and Wang, Q.: Source, long-range transport, and characteristics of a heavy dust pollution event in Shanghai, Journal of Geophysical Research Atmospheres, 115, 6128-6128, 2010.
Fu, X., Wang, S. X., Cheng, Z., Xing, J., Zhao, B., Wang, J. D., and Hao, J. M.: Source, transport and impacts of a heavy dust event in the Yangtze River Delta, China, in 2011, Atmospheric Chemistry & Physics, 14, 1239-1254, 2014.
Green, M. C., Chen, L. A., DuBois, D. W., and Molenar, J. V.: Fine particulate matter and visibility in the Lake Tahoe Basin: Chemical characterization, trends, and source apportionment, Journal of the Air & Waste Management Association, 62, 953-965, 2012.
Grundstrom, M., Tang, L., Hallquist, M., Nguyen, H., Chen, D., and Pleijel, H.: Influence of atmospheric circulation patterns on urban air quality during the winter, Atmospheric Pollution Research, 6, 278-285, 2015.
He, K., Yang, F., Ma, Y., Zhang, Q., Yao, X., Chan, C. K., Cadle, S., Chan, T., and Mulawa, P.: The characteristics of PM 2.5 in Beijing, China, Atmospheric Environment, 35, 4959-4970, 2001.
Ho, K. F., Lee, S. C., Chan, C. K., Yu, J. C., Chow, J. C., and Yao, X. H.: Characterization of chemical species in PM 2.5 and PM 10 aerosols in Hong Kong, Atmospheric Environment, 37, 31-39, 2003.
Huang, K., Zhuang, G., Lin, Y., Fu, J. S., Wang, Q., Liu, T., Zhang, R., Jiang, Y., Deng, C., Fu, Q., Hsu, N. C., and Cao, B.: Typical types and formation mechanisms of haze in an Eastern Asia megacity, Shanghai, Atmos. Chem. Phys., 12, 105-124, 2012.
Huang, R. J., Zhang, Y., Bozzetti, C., Ho, K. F., Cao, J. J., Han, Y., Daellenbach, K. R., Slowik, J. G., Platt, S. M., and Canonaco, F.: High secondary aerosol contribution to particulate pollution during haze events in China, Nature, 514, 218-222, 2014.
Huang, X., Wang, T., Talbot, R., Xie, M., Mao, H., Li, S., Zhuang, B., Yang, X., Fu, C., and Zhu, J.: Temporal characteristics of atmospheric CO2 in urban Nanjing, China, Atmospheric

Research, 153, 437-450, 2015.

Ji, D., Wang, Y., Wang, L., Chen, L., Hu, B., Tang, G., Xin, J., Song, T., Wen, T., and Sun, Y.: Analysis of heavy pollution episodes in selected cities of northern China, Atmospheric Environment, 50, 338–348, 2012.

Kanamitsu, M., Ebisuzaki, W., Woollen, J., Yang, S., Hnilo, J., Fiorino, M., and Potter, G.: NCEP-DOE AMIP-II reanalysis (R-2). Bulletin of the American Meteorological Society, Doibams, 2002.

Kang, H., Zhu, B., Su, J., Wang, H., Zhang, Q., and Wang, F.: Analysis of a long-lasting haze episode in Nanjing, China, Atmospheric Research, s 120–121, 78–87, 2013.

Kirchhofer, W,: Classification of European 500mb patterns, Arbeitsbericht der Schweizerischen Meteorologischen Zentralanstalt, Geneva, 43p, 1973.

Kappos, A. D., Bruckmann, P., Eikmann, T., Englert, N., Heinrich, U., Höppe, P., Koch, E., Krause, G. H., Kreyling, W. G., and Rauchfuss, K.: Health effects of particles in ambient air, International Journal of Hygiene & Environmental Health, 207, 399-407, 2004.

Kong, X., He, W., Qin, N., He, Q., Yang, B., Ouyang, H., Wang, Q., and Xu, F.: Comparison of transport pathways and potential sources of PM 10 in two cities around a large Chinese lake using the modified trajectory analysis, Atmospheric Research, 122, 284-297, 2013.

Kurokawa, J., Ohara, T., Morikawa, T., and Hanayama, S.: Emissions of air pollutants and greenhouse gases over Asian regions during 2000–2008: Regional Emission inventory in ASia (REAS) version 2, Atmospheric Chemistry & Physics, 13, 10049-10123, 2013.

Li, L., Chen, C. H., Fu, J. S., Huang, C., Streets, D. G., Huang, H. Y., Zhang, G. F., Wang, Y. J., Jang, C. J., and Wang, H. L.: Air quality and emissions in the Yangtze River Delta, China, Atmospheric Chemistry & Physics, 10, 1621-1639, 2011.

Li, Q., Zhang, R., and Wang, Y.: Interannual variation of the wintertime fog–haze days across central and eastern China and its relation with East Asian winter monsoon, International Journal of Climatology, 36, 346-354, 2016.

Mcgowan, H., and Clark, A.: Identification of dust transport pathways from Lake Eyre, Australia using Hysplit, Atmospheric Environment, 42, 6915-6925, 2008.

McGregor, G., and Bamzelis, D.: Synoptic typing and its application to the investigation of weather air pollution relationships, Birmingham, United Kingdom, Theoretical and Applied Climatology, 51, 223-236, 1995.

Malm, W. C., Sisler, J. F., Huffman, D., Eldred, R. A., and Cahill, T. A.: Spatial and seasonal trends in particle concentration and optical extinction in the United States, Journal of Geophysical Research: Atmospheres, 99, 1347-1370, 1994.

Ming, L., Ling, J., Li, J., Fu, P., Yang, W., Di, L., Gan, Z., Wang, Z., and Li, X.: PM 2.5 in the Yangtze River Delta, China: Chemical compositions, seasonal variations, and regional pollution events, Environmental Pollution, 223, 200, 2017.

Niu, F., Li, Z., Li, C., Lee, K. H., and Wang, M.: Increase of wintertime fog in China: Potential impacts of weakening of the Eastern Asian monsoon circulation and increasing aerosol loading, Journal of Geophysical Research: Atmospheres, 115, 2010.

Oanh N T K, Leelasakultum K.: Analysis of meteorology and emission in haze episode prevalence over mountain-bounded region for early warning, Science of the Total Environment, 409(11), 2261-2271, 2011.

Putaud, J.-P., Raes, F., Van Dingenen, R., Brüggemann, E., Facchini, M.-C., Decesari, S., Fuzzi, S., Gehrig, R., Hüglin, C., and Laj, P.: A European aerosol phenomenology—2: chemical characteristics of particulate matter at kerbside, urban, rural and background sites in Europe, Atmospheric environment, 38, 2579-2595, 2004

Rolph, G.: Real-time Environmental Applications and Display sYstem (READY) Website. Silver Spring, MD: NOAA Air Resources Laboratory, ready. arl. noaa. gov, 2013.

Russo, A., Trigo, R. M., Martins, H., and Mendes, M. T.: NO_2, PM_{10} and O_3 urban concentrations and its association with circulation weather types in Portugal, Atmospheric Environment, 89, 768-785, 2014.

Santurtún, A., González-Hidalgo, J. C., Sanchez-Lorenzo, A., and Zarrabeitia, M. T.: Surface ozone concentration trends and its relationship with weather types in Spain (2001–2010), Atmospheric Environment, 101, 10-22, 2015.

Shan, W., Yin, Y., Lu, H., and Liang, S.: A meteorological analysis of ozone episodes using HYSPLIT model and surface data, Atmospheric Research, 93, 767-776, 2009.

Singh, A., and Dey, S.: Influence of aerosol composition on visibility in megacity Delhi, Atmospheric Environment, 62, 367-373, 2012.

Shu, L., Xie, M., Wang, T., Chen, P., Han, Y., Li, S., Zhuang, B., Li, M., and Gao, D.: Integrated studies of a regional ozone pollution synthetically affected by subtropical high and typhoon system in the Yangtze River Delta region, China, 1-32, 2016.

State Environmental Protection Administration of China, 2006. China National Environmental Protection Standard: Automated Methods for Ambient Air Quality Monitoring. China Environmental Science Press, Beijing.

Stein, A. F., Draxler, R. R., Rolph, G. D., Stunder, B. J. B., Cohen, M. D., and Ngan, F.: NOAA's HYSPLIT Atmospheric Transport and Dispersion Modeling System, Bulletin of the American Meteorological Society, 96, 150504130527006, 2016.

Wang, Y., Stein, A. F., Draxler, R. R., Rosa, J. D. D. L., and Zhang, X.: Global sand and dust storms in 2008: Observation and HYSPLIT model verification, Atmospheric Environment, 45, 6368-6381, 2011.

Wang, J., Hu, Z., Chen, Y., Chen, Z., and Xu, S.: Contamination characteristics and possible sources of PM10 and PM2.5 in different functional areas of Shanghai, China, Atmospheric Environment, 68, 221-229, 2013.

Wang, Y., Li, L., Chen, C., Huang, C., Huang, H., Feng, J., Wang, S., Wang, H., Zhang, G., and Zhou, M.: Source apportionment of fine particulate matter during autumn haze episodes in Shanghai, China, Journal of Geophysical Research Atmospheres, 119, 1903–1914, 2014.

Wang, M., Cao, C., Li, G., and Singh, R. P.: Analysis of a severe prolonged regional haze episode in the Yangtze River Delta, China, Atmospheric Environment, 102, 112-121, 2015.

Xie, M., Zhu, K., Wang, T., Yang, H., Zhuang, B., Li, S., Li, M., Zhu, X., and Ouyang, Y.: Application of photochemical indicators to evaluate ozone nonlinear chemistry and pollution control countermeasure in China, Atmospheric Environment, 99, 466-473, 2014.

Xie, M., Liao, J., Wang, T., Zhu, K., Zhuang, B., Han, Y., Li, M., and Li, S.: Modeling of the anthropogenic heat flux and its effect on regional meteorology and air quality over the Yangtze River Delta region, China, Atmospheric Chemistry & Physics, 16, 6071-6089, 2016a.

Xie, M., Zhu, K., Wang, T., Chen, P., Han, Y., Li, S., Zhuang, B., and Shu, L.: Temporal characterization and regional contribution to O_3 and NO_x at an urban and a suburban site in Nanjing, China, Science of the Total Environment, 551, 533-545, 2016b.

Xie, M., Zhu, K., Wang, T., Feng, W., Li, M., Li, M., Han, Y., Li, S., Zhuang, B., and Shu, L.: Changes of regional meteorology induced by anthropogenic heat and their impacts on air quality in South China, Atmospheric Chemistry & Physics, 16, 15011-15031, 2016c.

Xie, M., Shu, L., Wang, T.-j., Liu, Q., Gao, D., Li, S., Zhuang, B.-l., Han, Y., Li, M.-m., and Chen, P.-l.: Natural emissions under future climate condition and their effects on surface ozone in the Yangtze River Delta region, China, Atmospheric Environment, 150, 162-180, 2017.

Xu, J. S., Xu, H. H., Xiao, H., Tong, L., Snape, C. E., Wang, C. J., and He, J.: Aerosol composition and sources during high and low pollution periods in Ningbo, China, Atmospheric Research, s 178–179, 559-569, 2016.

Yan, X. Y., Ohara, T., and Akimoto, H.: Bottom-up estimate of biomass burning in mainland China, Atmospheric Environment, 40, 5262-5273, 2006.

Yang, S., He, H., Lu, S., Chen, D., and Zhu, J.: Quantification of crop residue burning in the field and its influence on ambient air quality in Suqian, China, Atmospheric Environment, 42, 1961-1969, 2008.

Yarnal, B.: A procedure for the classification of synoptic weather maps from gridded atmospheric pressure surface data, Computers & Geosciences, 10, 397-410, 1984.

Young, D. E., Kim, H., Parworth, C., Zhou, S., Zhang, X., Cappa, C. D., Seco, R., Kim, S., Zhang, Q.: Influences of emission sources and meteorology on aerosol chemistry in a polluted urban environment: results from DISCOVER-AQ California, Atmospheric Chemistry and Physics, 16(8), 5427-5451, 2016.

Zhang, J. P., Zhu, T., Zhang, Q. H., Li, C. C., Shu, H. L., Ying, Y., Dai, Z. P., Wang, X., Liu, X. Y., and Liang, A. M.: The impact of circulation patterns on regional transport pathways and air quality over Beijing and its surroundings, Atmospheric Chemistry & Physics, 11, 33465-33509, 2012.

Zhang, Q., Quan, J., Tie, X., Li, X., Liu, Q., Gao, Y., and Zhao, D.: Effects of meteorology and secondary particle formation on visibility during heavy haze events in Beijing, China, Science of the Total Environment, 502C, 578-584, 2014.

Zhao, X. J., Zhao, P. S., Xu, J., and Meng, W.: Analysis of a winter regional haze event and its formation mechanism in the North China Plain, Atmospheric Chemistry & Physics, 13, 5685-5696, 2013.

Zheng, G., Duan, F., Su, H., Ma, Y., Cheng, Y., Zheng, B., Zhang, Q., Huang, T., Kimoto, T., and Chang, D.: Exploring the severe winter haze in Beijing: the impact of synoptic weather, regional transport and heterogeneous reactions, Atmospheric Chemistry and Physics, 15, 2969-2983, 2015a.

Zheng, X. Y., Fu, Y. F., Yang, Y. J., and Liu, G. S.: Impacts of atmospheric circulations on aerosol distributions in autumn over eastern China: observational evidences, Atmospheric Chemistry & Physics, 15, 3285-3325, 2015b.

Zhu, J., Wang, T., Deng, J., Jiang, A., and Liu, D.: An emission inventory of air pollutants from crop residue burning in Yangtze River Delta Region and its application in simulation of a heavy haze weather process, Acta Scientiae Circumstantiae, 32, 3045-3055, 2012.

Zhu, K., Xie, M., Wang, T., Cai, J., Li, S., and Feng, W.: A modeling study on the effect of urban land surface forcing to regional meteorology and air quality over South China, Atmospheric Environment, 152, 389-404, 2017.

Zhuang, G. S., Yuan, J. H., Yuan, H., Zhao, C. Y.: The compositions, sources, and size distribution of the dust storm from China in spring of 2000 and its impact on the global environment, Science Bulletin, 46, 895-901, 2001.